Investigation of Immersed Coil Heat Exchangers in regard to Heat Transfer and Storage Stratification

William Logie*, Elimar Frank, Michel Y. Haller and Matthias Rommel

Institute für Solartechnik SPF, HSR Hochschule für Technik, Oberseestr. 10, 8640 Rapperswil, Switzerland

* Phone: +41 55 222 4834, Email: william.logie@solarenergy.ch

Abstract

Current implementation of Immersed Coil Heat Exchangers (IHX) into Solar Domestic Hot Water (SDHW) systems use simple guidelines for dimensioning their surface area based on an intended solar collector area - or range thereof. The literature from whence these guidelines come (1970s and 80s) are based on experiments with different types of IHX (copper, flange-retrofitted) to those used today and are evaluated solely on the performance of heat transfer, thus a re-evaluation of these guidelines is considered necessary. The investigations presented attempt to combine an evaluation of the heat transfer performance and stratification together based on measurements from three IHX samples with varying material and geometrical arrangement. Preliminary analysis suggests a correlation between high convective heat transfer coefficients and low stratification efficiencies.

1. Introduction

Observing the solar Thermal Energy Storage (TES) market one recognises a strong presence of immersed coil heat exchangers in systems smaller than 1000 litres. This has its reasons in the cost of production, whereby depending on the material chosen, the competitiveness of external heat exchangers takes over in systems of greater size or higher performance (stratification devices).

Based on in situ measurements it has been shown that low flow collector operation leads to better stratification in the IHX occupied region of a SDHW TES, which in turn decreases the amount of primary energy (-5.2%) required to maintain hot water temperature and drive the circulation pump [1]. In addition, simulation sensitivity analysis parameterised from these measurements indicated that a significant variation (±50%) in the IHX heat transfer coefficient has but a small influence on the annual solar gain of the system (±2%). Although many studies of natural convective heat transfer have been performed on immersed coil heat exchangers over the past 30 years, their performance in SDHW systems is not fully understood, partially because heat transfer and storage stratification were not considered in parallel.

The dimensioning and positioning of the IHX so as to inhibit mixing in the TES and maintain heat transfer effectiveness - if not improve thereon – seems possible [2]. The aim of these investigations is to quantify an answer in a controlled laboratory environment.

2. Investigations

In the first phase of investigations fifty conventional SDHW systems in the order of 350 to 450 litres were inspected for geometry of tank and heat exchanger [3]. The significant variation in heat exchanger parameters was found to have mild correlation to collector surface area and be limited by the dimensions of the tank mantel. It is understood as a result that while certain parameters like tube diameter vary little, surface area or the positioning of the coil within the tank varies much. Being something hard to predict it is assumed that other factors in the design process take precedence and only heat exchanger surface area is maximised.

With the help of TRNSYS simulations a 400ℓ reference SDHW system was defined and its annual operation under high and low flow was analysed to determine the most important conditions under which a solar connected IHX operates [3].

Based on these studies a suitable laboratory with specially constructed stainless steel TES (diameter 650 mm), a pre-conditioning circuit and a solar IHX charging source was assembled. The experiments are observed on the one hand through calibrated calorimetric measurements (magnetic flow meter and 4-wire Pt-100 temperature sensors) and on the other hand through windows by the quantitative flow visualisation methods of Particle Image Velocimetry (PIV) and Laser Induced Fluorescence (LIF). The later hand allows one to gain insight into mixing and temperature distribution in a two dimensional spatial and temporal domain (at a radial cross section of the tank) without disturbing the fluid dynamics (although the addition of windows to a cylindrical TES raises a question of integrity).

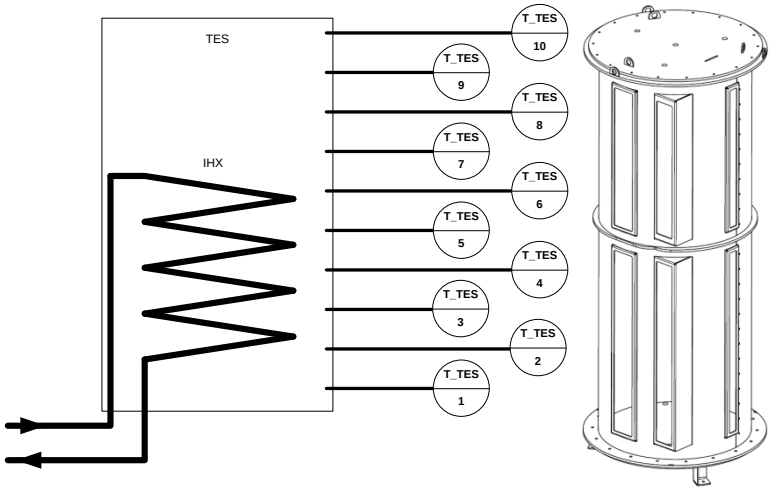

Figure 1: The TES is installed with 10 Pt-100 sensors over its height and insulated with 70 mm insulation material (except for the observation windows)

To date constant IHX power (1 and 2 kW) and flow rate (70, 200 and 350 kg/hr) experiments have been performed on three differing IHX samples from the market. These flow rates inside the IHX correspond to area-specific flow rates in the solar loop of approximately 10, 30 and 50 kg/h per m^2 collector area if a total collector area of $7m^2$ is assumed. Important details of the IHX samples can be read from Table 1.

Table 1: Properties of the three heat exchangers tested

Property description	Units	A	B	C
IHX Form	-	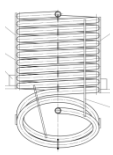	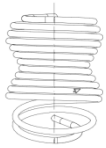	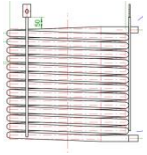
Material	-	Crude steel (enamelled)	Stainless steel	Crude steel (enamelled)
Material conductance λ	W/m.K	~ 30	~ 15	~ 30
Coil diameter *D*	mm	440	400	490
Coil height *H*	mm	650	600	470
Coil pitch *p*	mm	45.0	35.0	36.2
Inner tube diameter d_i	mm	27.5	28.4	21.6
Outer tube diameter d_o	mm	35.0	30.0	26.9
IHX outer Area A_{IHX}	m^2	1.76	1.59	1.69
IHX coil Length *L*	m	16.6	16.9	20.0

Starting with a constant temperature of 20°C the TES was charged through the IHX until a temperature of 55°C was reached at TES Sensor 7. This is where a temperature sensor for controlling the auxiliary heating to maintain hot water temperature would be found. The IHX were run with a mixture of 33% glycol/67% water.

The question of how performance of the IHX and stratification is to be analysed requires a number of assumptions. For one, the temperature profile over the height of the TES is interpolated linearly between sensors. The rate of heat transferred can be calculated based on the measured quantities of mass flow $\dot{m}$, specific heat c_p and inlet and outlet temperatures ϑ as per Eq. (1).

$$\dot{Q} = \dot{m} c_p (\vartheta_{in} - \vartheta_{out}) \quad (1)$$

For an overall approximation of the heat transfer properties we begin with the bulk IHX temperature (average between inlet and outlet) from which an evaluation of the *forced convective* heat transfer coefficient inside the IHX h_i is obtained iteratively together with the inside IHX wall temperature using the Nusselt correlation from Gnielinski [4] and the relationship in Eq. (2) – where d_i is inside tube diameter and λ_{G/H_2O} is thermal conductivity of the glycol/water mix.

$$h_i = \frac{Nu_i \lambda_{G/H_2O}}{d_i} \quad (2)$$

This is known to be accurate to within ±15% for both laminar and turbulent conditions. The temperature difference across the tube wall (d_o is outside tube diameter) is then determined using Eq. (3) over the length of the tube L_{IHX} .

$$d\vartheta_w = \frac{\dot{Q} \cdot \ln\left(\frac{d_o}{d_i}\right)}{2\pi\lambda_{IHX} L_{IHX}} \tag{3}$$

The external *free convective* heat transfer coefficient results from the remaining temperature difference between the outside wall temperature ($\vartheta_{w,o}$) and the temperatures measured inside the TES of the free fluid around the IHX by way of Eq. (4) and analogous to Eq. (2).

$$Nu_o = \frac{\dot{Q} d_o}{\lambda_{H_2O} A_{IHX} \cdot (\vartheta_{w,o} - \vartheta_{TES})} \tag{4}$$

Local fluctuations within temperatures around the coil were sought from LIF measurements; specifically the temperature gradients from the coils outer surface towards the TES free fluid. To date precise LIF measurements have proved to be elusive (at best ±2K uncertainty) and as such only the global calorimetric measurements are presented here.

A number of publications have discussed approaches for the evaluation of stratification in TES [5], the most comprehensive of which requires the balancing of entropy across the system boundary marked by the walls of the TES [6,7]. Balancing between energy gains and losses and for measurement inaccuracies, the generation of entropy in each run was calculated with the method from [6], giving expression to the irreversible processes (from mixing and heat exchange) in the form of irreversible entropy ($S_{irr,exp}$). Differing slightly from this method is how the irreversible entropy generated was compared to some *best* or *worst* case scenario, which is necessary for determining an arbitrary measure of how good the *real* situation is. For simplicity it was assumed that the theoretical fully mixed tank received the same amount of energy from the IHX as the real case and that losses were also considered identical to the real case. The generation of entropy in the mixed scenario ($S_{irr,mix}$) is then calculated for a single TES temperature. As in [6] the so called stratification efficiency is calculated by way of Eq. (5).

$$\zeta_{S_{irr}} = 1 - \frac{S_{irr,exp}}{S_{irr,mix}} \tag{5}$$

The generation of entropy is observed from the beginning to the end of each run which is why constant operating conditions (power and mass flow) are ensured.

3. Results

The results are tabulated for a charging power of 2kW and flow rates of 70 and 350kg/hr in Table 2 and Table 3 respectively. All values are averaged over the charging period covering a range of temperatures in the IHX and TES from 20 to 70°C.

Table 2: IHX performance for a charging power of 2 kW and flow rate of 70kg/hr

Evaluated property	Units	A	B	C
Inner Reynolds number Re_i	-	527	665	867
Flow type inside tube	-	laminar	laminar	laminar
Inside Nusselt number	-	53.9	60.6	76.2
Outside Nusselt number	-	5.4	5.8	4.6
Inside heat transfer coefficient h_i	W/m^2.K	882	1003	1653
Outside heat transfer coefficient h_o	W/m^2.K	96	121	108
IHX overall *U*-value	W/m^2.K	83	107	99
Stratification efficiency ζ	%	4.1	1.5	2.1

Table 3: IHX performance for a charging power of 2 kW and flow rate of 350kg/hr

Evaluated property	Units	A	B	C
Inside Reynolds number Re_i	-	3080	2921	3772
Flow type inside IHX	-	laminar	laminar	laminar
Inside Nusselt number	-	266.0	254.4	319.7
Outside Nusselt number	-	10.6	13.8	10.6
Inside heat transfer coefficient h_i	W/m^2.K	4540	4185	6857
Outside heat transfer coefficient h_o	W/m^2.K	191	288	249
IHX overall *U*-value	W/m^2.K	176	264	232
Stratification efficiency ζ	%	2.0	0.5	2.0

Furthermore we can visualise in plots the dependency of IHX performance on mass flow in Figure 2, in which the overall heat transfer area coefficient is shown, and Figure 3 where the internal and external convective heat transfer coefficients are shown.

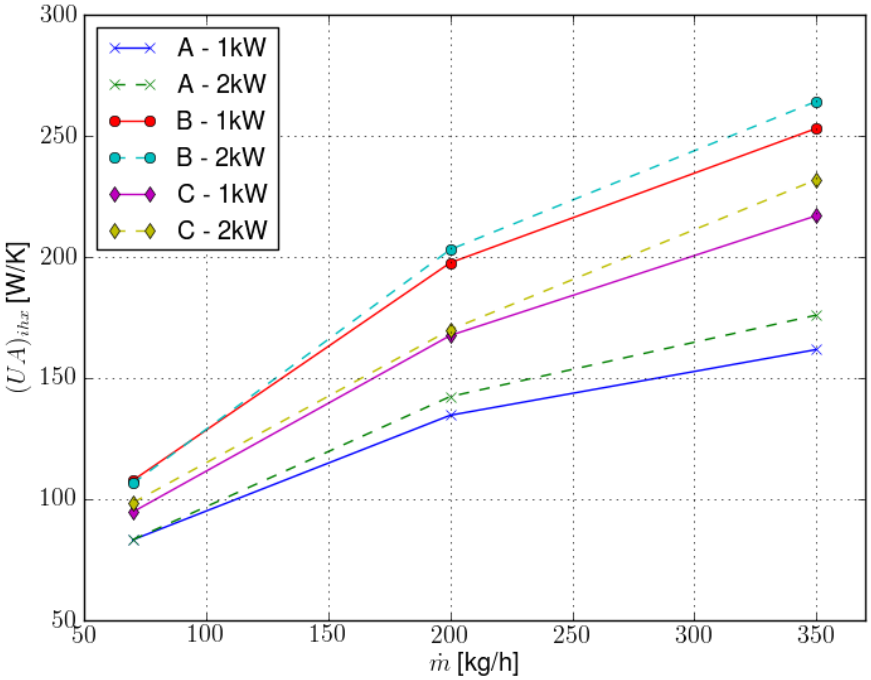

Figure 2: Plot of overall heat transfer area coefficient against mass flow

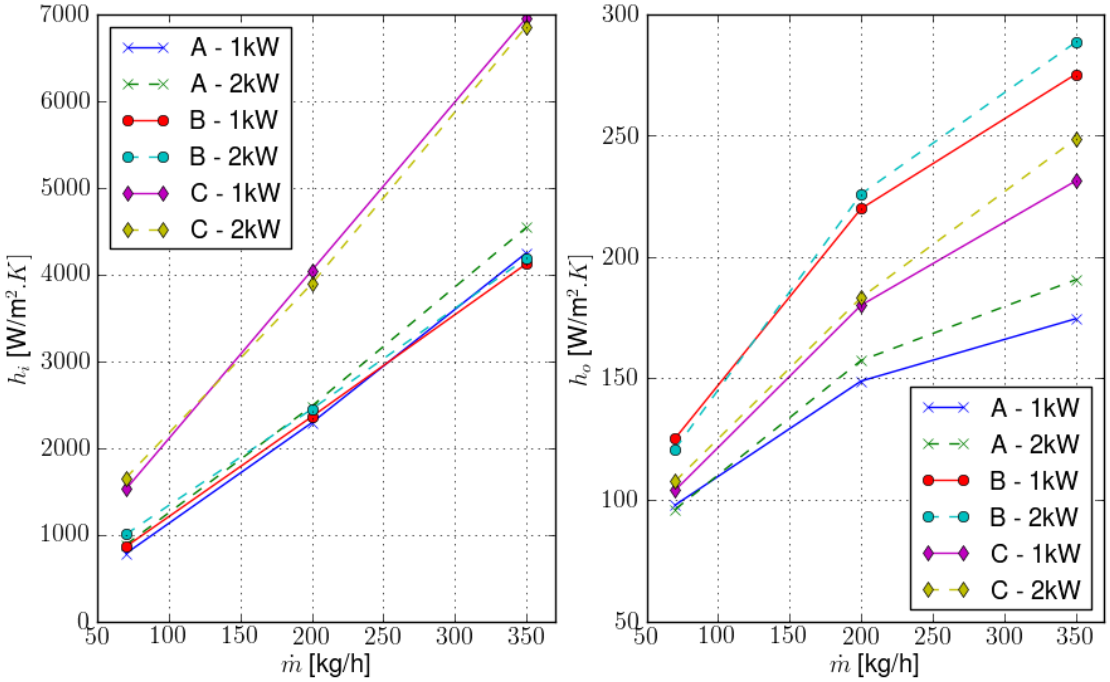

Figure 3: Plot of internal (left) and external (right) *convective* heat transfer coefficient against mass flow

Judging by the overall heat transfer area coefficient (Figure 2) we see that IHX B has the highest heat transfer area coefficient. This is due to its strong free convective component as can be seen from Figure 3, right hand side. The smaller tube diameter of IHX C induces stronger internal forced convection which is why it performs better than IHX A.

From work mentioned earlier [2] we know that the external Nusselt number is highest at the bottommost turn of the IHX because there is no tubing below it whose plume and associated higher temperature inhibits the transfer of heat. As the plume rises and flows around each tube above, the local Nusselt number for the turn in question is reduced [2]. It is safe to assume that the high heat transfer area coefficient of IHX B is due to the varying coil diameter which separates such plumes from the tubing above. The thinner wall thickness of IHX B allows more temperature gradient in the storage water which would induce mildly higher convection. The reason IHX C has a higher heat transfer area coefficient than IHX A is the fact that ¾-inch tubing is used instead of 1-inch tubing. Although decreasing tube diameter would seem at first glance to make sense, one must consider the higher pressure drop and pump energy associated with this decision.

To speak of stratification where IHXs are used is optimistic, seeing as we are at best attaining some level of stratification in the volume of TES occupied by the IHX - if at all. The highest stratification efficiency reached was IHX A with barely 4% (low-flow). The results help to confirm the intuitive idea that higher external convective forces lead to more mixing of the TES, illustrated for all experiments in Figure 4 with a decreasing trend in stratification efficiency for higher external convection conditions (Nusselt numbers).

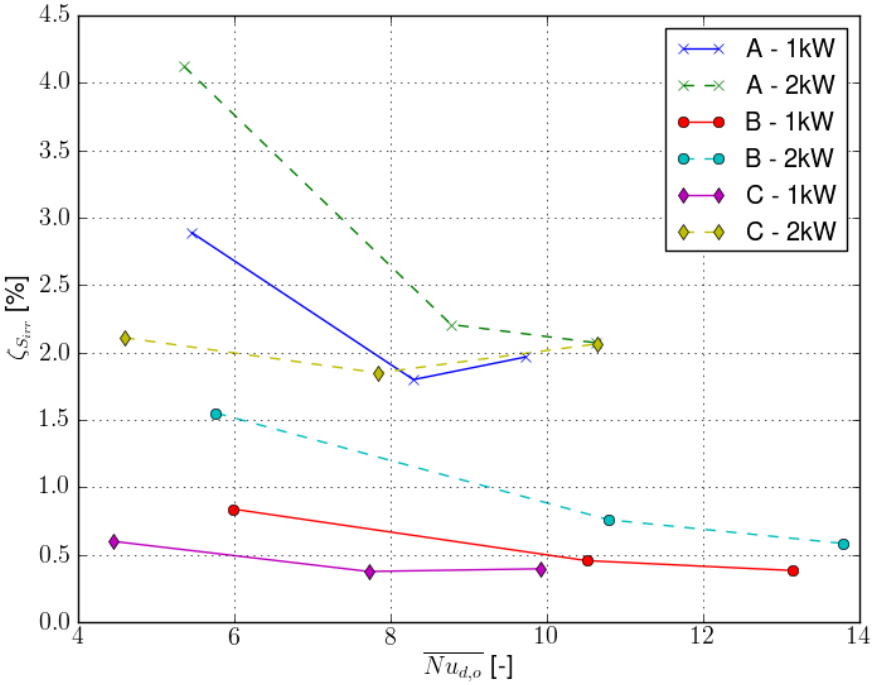

Figure 4: Plot of all IHX experiments showing the relationship between stratification efficiency and external heat convection (Nusselt number). A mild asymptotic trend is visible.

4. Conclusion

The investigations presented here confirm a number of things:

- increased flow-rate over an IHX improves convective heat transfer but disrupts the mild stratification in the bottom of a SDHW TES,
- the geometry of an IHX influences both its convective heat transfer performance and effect to stratification, but
- the parameterisation of heat exchanger performance based on geometry is complicated and requires measurements with sufficient resolution in the operating conditions and variation over each geometric parameter individually.

The difficulty in disseminating such results lies in their specific nature, as often a storage tank is conceived for a certain range of collector field areas rather than for one specific fixed area. The results presented here encompass the *base case* of contemporary IHX design and implementation, from which a number of sensitivity studies shall be made.

5. References

[1] J. Scheuren, F. Pujiula, W. Eisenmann, W. Böhle, and B. Hafner, "Comparitive Measurements of two Identical Solar Systems with High-flow and Low-flow Rates," in *EUROSUN*, Freiburg, 2004, pp. 236-242.

[2] H. Messerschmid, "Entwicklung und Validation eines numerischen Verfahrens zur Beurteilung von Trinkwasserspeichern," PhD Thesis 2002.

[3] W. R. Logie and E. Frank, "Potential improvement in the design of immersed coil heat exchangers," in *ISES Solar World Congress*, Johanessburg, 2009, pp. 717-716.

[4] Y. Gnielinski, "Heat transfer and pressure drop in helically coiled tubes," in *Heat Transfer 1986*, San Francisco, USA, 1986, pp. 2847-2854.

[5] M. Y. Haller et al., "Methods to determine stratification efficiency of thermal energy storage process - Review and theoretical comparison," *Solar Energy*, vol. 83, pp. 1847-1860, 2009.

[6] M. Y. Haller et al., "A method to determine stratification efficiency of thermal storage process independently from storage heat losses," *Solar Energy*, vol. 84, pp. 997-1007, 2010.

[7] E. Hahne, R. Kübler, and J. Kallweit, "The evaluation of Thermal Stratification by Exergy," in *Energy Storage Systems (Editors: B. Kilkis and S. Kakac)*, Dortrecht, 1989, pp. 465-485.

6. Errata

Due to a glitch in the iteration for internal Nusselt number, significantly higher values were reported and as such the external values were small. In subsequent analysis the mistake came to air and has been corrected. Comparison between test subjects remains the same within the scope of this paper, the scale however on which this comparison occurs has changed, therefore the relevant tables and figures are reproduced below.

Table 2: IHX performance for a charging power of 2 kW and flow rate of 70kg/hr

Evaluated property	Units	A	B	C
Inner Reynolds number Re_i	-	592	665	867
Flow type inside tube	-	laminar	laminar	laminar
Inside Nusselt number	-	17.5	18.4	19.2
Outside Nusselt number	-	7.4	8.2	6.1
Inside heat transfer coefficient h_i	W/m^2.K	287	305	417
Outside heat transfer coefficient h_o	W/m^2.K	133	171	142
IHX overall *U*-value	W/m^2.K	145	169	166
Stratification efficiency ζ	%	4.1	1.5	2.1

Table 3: IHX performance for a charging power of 2 kW and flow rate of 350kg/hr

Evaluated property	Units	A	B	C
Inside Reynolds number Re_i	-	3080	2921	3772
Flow type inside IHX	-	laminar	laminar	laminar
Inside Nusselt number	-	45.1	45.8	47.1
Outside Nusselt number	-	14.5	21	15.7
Inside heat transfer coefficient h_i	W/m^2.K	768	753	1009
Outside heat transfer coefficient h_o	W/m^2.K	259	440	367
IHX overall *U*-value	W/m^2.K	307	420	392
Stratification efficiency ζ	%	2.0	0.5	2.0

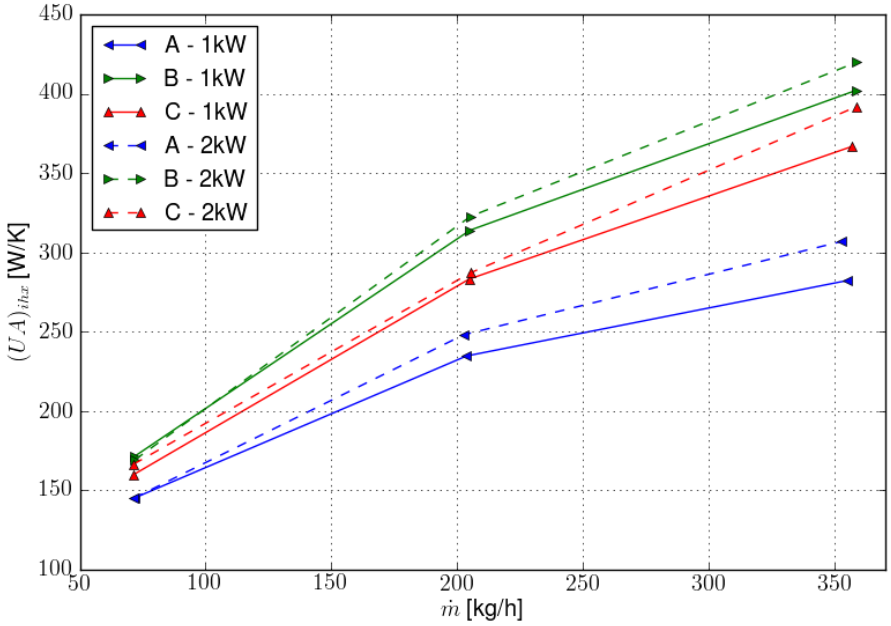

Figure 2: Plot of overall heat transfer area coefficient against mass flow

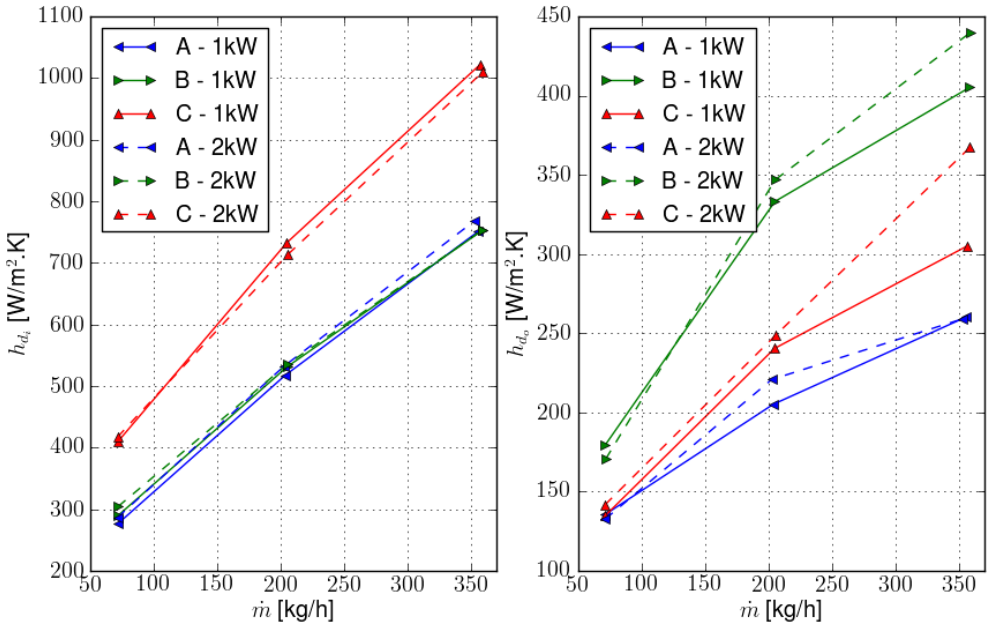

Figure 3: Plot of internal (left) and external (right) convective heat transfer coefficient against mass flow

William Logie, 12th December 2010.